MICROWAVE EMISSION FROM POLAR SURFACES

Final Report

1 April 1998

19980505 163

Thomas C. Grenfell
Department of Atmospheric Sciences, University of Washington
Seattle, Washington 98195-1640
e-mail: tcg@atmos.washington.edu
Phone: 206-543-9411 Fax: 206-543-0308
Grant Number: N00014-96-1-0324

GOALS and OBJECTIVES

Our long term goals for this project have been to understand the relationships between spectral microwave emissivity signatures from centimeter to millimeter wavelengths and the physical, structural, and optical properties of Arctic and Antarctic sea ice. This has provided fundamental information for determining how effectively multifrequency multipolarization passive microwave satellite data can be used to identify the spatial and temporal distribution of the different types, ages and surface temperatures of sea ice. During the research carried out under the present funding by the Office of Naval Research we have concentrated on determining and understanding the microwave signatures of new and young ice from initial formation through to the development of thick first-year ice. Ice types in this range are difficult to resolve from space, but they play a major role in the transfer of energy between the polar oceans and the atmosphere. At the same time we have broadened our scope to include a comparison of the passive microwave signatures with radar, visible, and infrared in order to be able to combine the information from a wide variety of satellite sensors in a consistent fashion.

Because of the importance of new and young ice types for the regional energy balance and dynamical behavior of the ice covered oceans, our principal objective has been to investigate the temporal dependence of combined electromagnetic signatures of sea ice types from open water and new ice through thick first-year ice to relate this dependence to changes in the physical properties of the ice via direct theoretical modeling. We have been concentrating in particular on the growth of thin congelation and frazil/pancake ice, with special emphasis on the transition from young ice to first-year ice. Other cases of direct interest in which we have participated include investigations of (1) the influence of a snow cover on thin ice, (2) bare versus snow-covered thick first-year ice, (3) the contrast between the signatures of congelation and frazil/pancake ice, and (4) the effects of deformed or ridged ice. Because we now have available detailed observations of the physical properties of the ice for these cases, it is now practical to include these results in suitable direct theoretical models to predict electromagnetic signatures. Our goal in this respect has been to use our models with consistent sets of input data to compare predicted and observed electromagnetic signatures.

APPROACH

Our approach has been to compare the results of our observations with the results of our theoretical models to provide a causal link between the physical properties of sea ice and the way it interacts with

REPORT DOCUMENTATION PAGE

Form Approved OMB No. 0704-0188

1. AGENCY USE ONLY *(Leave blank)*

2. REPORT DATE 1 April 1998

3. REPORT TYPE AND DATES COVERED Final Report 1 Oct 95 - 30 Sept 97

4. TITLE AND SUBTITLE Microwave Emission from Polar Surfaces

5. FUNDING NUMBERS G N00014-96-1-0324

6. AUTHOR(S) Thomas C. Grenfell

7. PERFORMING ORGANIZATION NAME(S) AND ADDRESS(ES)
Department of Atmospheric Sciences
Box 351640
University of Washington
Seattle WA 98195-1640

8. PERFORMING ORGANIZATION REPORT NUMBER 61-6612

9. SPONSORING / MONITORING AGENCY NAME(S) AND ADDRESS(ES) Office of Naval Research

10. SPONSORING / MONITORING AGENCY REPORT NUMBER

11. SUPPLEMENTARY NOTES

a. DISTRIBUTION / AVAILABILITY STATEMENT No limitation

12. DISTRIBUTION CODE

13. ABSTRACT *(Maximum 200 words)*

Based on the work described in this report, our observations and modeling work have revealed several considerations which are central to understanding the physical basis for the application and interpretation of thin ice algorithms for passive microwave imagery. We have shown that passive microwave measurements provide one of the most robust remote sensing techniques for distinguishing among sea ice types - including the thin ice types that are pivotal for regional energy considerations. We have found that current theories applicable at microwave frequencies (multilayer SFT wave theory, for example) and in the visible and infrared (radiative transfer theory) can reproduce the radiation signatures of FY ice types quite well incorporating the actual physical structure of the ice. As a result of the cooperative work carried out during the electromagnetics ARI, the determination of the wavelength regions and physical situations appropriate for the application of various radiation models has been improved considerably, and our results, both theoretical and observational, have demonstrate the levels of accuracy of the models. It is clear that our understanding of the microwave emissivities of sea ice and their relation to other types of remote sensing signatures has increased significantly in the course of this grant.

14. SUBJECT TERMS Microwave, emissivity, brightness temperature, sea ice, new ice, young ice, spectral albedo, radar backscatter, infrared emissivity, radiative transfer, wave theory

15. NUMBER OF PAGES 11

16. PRICE CODE

17. SECURITY CLASSIFICATION OF REPORT	18. SECURITY CLASSIFICATION OF THIS PAGE	19. SECURITY CLASSIFICATION OF ABSTRACT	20. LIMITATION OF ABSTRACT
None	None	None	SAR

electromagnetic radiation (apparent optical properties). To this end we have compiled the passive microwave and thermal infrared observations of sea ice from all of our recent field experiments in order to refine our estimates of the signature evolution in selected two dimensional parameter spaces: for example e[18.7GHz,V-Pol] versus e[37GHz,V-Pol]) and PR versus GR (See figure 1). Over the past five years, we have extended our scope to incorporate into the comparison active microwave, visible/near-infrared observations, physical and biological observations obtained concurrently at the CRREL pond and at Pt. Barrow. We have developed appropriate forward radiation interaction models for each wavelength range and measurement type.

Our core data set consists of surface- based measurements of brightness temperature (T_B) and emissivity at microwave frequencies of 6.7, 10, 18.7, 37, 90 GHz for vertical and horizontal polarization (V-Pol & H-Pol) and in the thermal infrared (8-14μm band - unpolarized). Angular scans are available at selected sites from 30-70° nadir angle, and spatial scans at 50° nadir angle are available at 1 to 2 meter resolution. Corresponding radar data consisting of C, X, K and Ka-Band radar observations have been obtained by S. Nghiem and R. G. Onstott. The optical data consist of spectral albedos from 400 to 1000 nm obtained by D. K. Perovich. Ice sheet characterization data consist of bulk properties – typically salinity, density, and temperature depth profiles - and microscopic scale properties related to the size distributions and correlation functions for brine pockets and vapor bubbles. These data were provided by D. K. Perovich and A. J. Gow. Particular and dissolved matter concentrations have been provided by C. Roesler.

During the last 5 years we have investigated primarily the growth phases of congelation and pancake ice, the transition from new to young to first-year (FY) ice. We have also studied the properties of Arctic multiyear ice; however, considerable study is still needed to provide a general characterization of this ice type. We have concentrated on the relative importance of the near surface layers for both smooth ice and ice with a rough surface and/or a snow cover.

The first of the theoretical models we have used is a multilayer strong fluctuation theory (SFT) code based on the wave theory formulation of Stogryn for microwave permittivity, emissivity and volume scattering for inhomogeneous random media with strong permittivity fluctuations. Our other model is a multilayer multispectral discrete ordinates radiative transfer model that is applicable in the ultraviolet, visible, and thermal infrared.

WORK COMPLETED

Our most recent results are based primarily on a compilation and analysis of our data sets from seven field experiments carried out under ONR and NASA auspices (CEAREX 88-89, LEADEX 1992; CRREL 1993, 1994, & 1995; Beaufort & Chukchi Seas 1994; SIMMS 1995). These studies cover essentially all stages in the development of new, young, and first-year sea ice. In the past year, we have made significant contributions to the production of eight scientific papers involving various research themes of the electromagnetics ARI including a detailed study of the temporal evolution of electromagnetic signatures from initial formation through FY ice. We have cooperated with all the participants to exchange the data needed to build up the individual multisensor data sets. We have also successfully compared our model results with selected test cases and identified the important structural features of the ice that influence its electromagnetic signatures. These papers are currently under review and will appear in IEEE Transactions of Geoscience and Remote Sensing.

SUMMARY OF RESULTS

A variety of comparative results have been obtained among the electromagnetic signatures of new and young ice. Figure 1 shows the general evolutionary sequence in PR-GR space from open water through young ice for both congelation ice and frazil/pancake ice. PR-GR space is used to define the Goddard team algorithm for determining sea ice type. It is defined in terms of selected brightness temperature observations, T_B, by PR = $[T_B(18.7\text{,V-pol})-T_B(18.7\text{,H-pol})]/[T_B(18.7\text{,V-pol})+T_B(18.7\text{,H-pol})]$ and GR = $[T_B(37\text{,V-pol})-T_B(18.7\text{,V-pol})]/[T_B(37\text{,V-pol})+T_B(18.7\text{,V-pol})]$. These results have been produced from a compilation of the observations obtained from a variety of field experiments as noted in the figure legends. The picture that emerges is that the signature development for these frequencies is significantly different during the early stages for frazil/pancake ice, grown under wavy conditions, and congelation ice, grown when the water is calm. When the ice thickness increases to a few 10's of centimeters it is classified as young ice and the pancake ice tends to consolidate into a solid sheet. At this point, the GR values are essentially the same and the PR values are similar but tend to be slightly higher for the pancake ice.

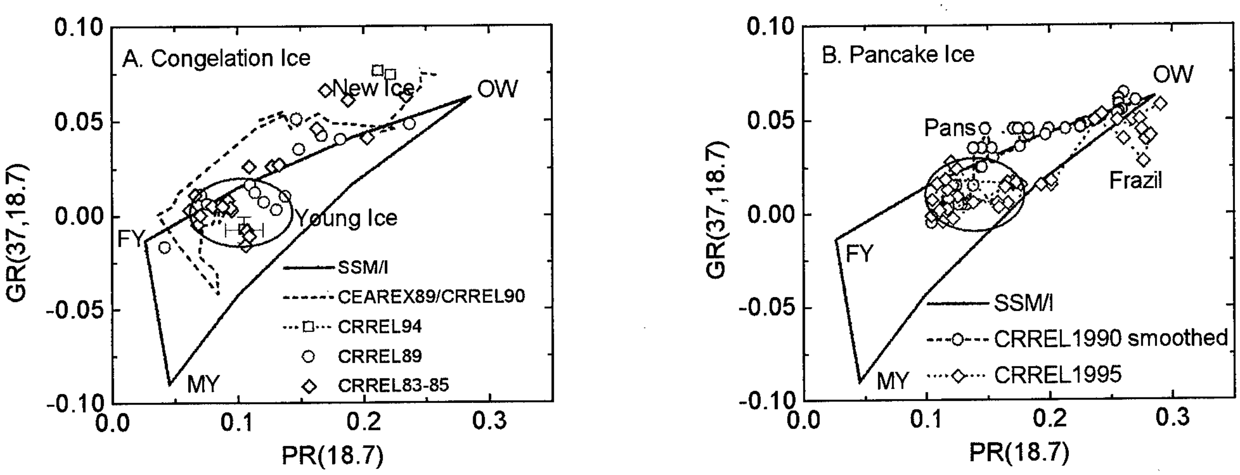

Fig. 1. GR-PR data from various experiments showing the signature evolution from open water through young ice for both congelation (A) and pancake ice (B). The ellipses show the regions of convergence for young ice.

Subsequent development as the ice thickens further and acquires a snow or frost flower cover is shown in figure 2. The evolution is almost the same from both congelation and pancake ice. During this process GR remains essentially unchanged while PR decreases to about 0.02 in, the value of thick first-year (FY) ice. The categorization of this behavior has made it possible to determine the concentration of thin (new & young) ice in marginal ice zones such as the Bering Sea. It also explains many of the uncertainties arising from previous interpretations of sea ice concentration from satellite imagery.

The behavior of sea ice emissivity at higher frequency (90 GHz) is illustrated in Figure 3 which shows a scatter plot of emissivity at 18.7GHz, vertical polarization (V) versus 90 GHz V-polarization. In this case, the both emissivities increase rapidly from the values for calm open water up to the bare ice region. For bare ice, the emissivities lie in a small region near the coordinates (0.92, 0.94). When snow is deposited onto the ice, however, it creates an inhomogeneous distribution of snow crystal sizes up to 1-2 mm across. This produces a significant amount of scattering at 90GHz which influences e(90V) and causes the emissivities to spread out over a rather wide range as shown. At 18.7 GHz the wavelength is sufficiently large that the scattering effect is negligible and the range of values remains essentially unchanged.

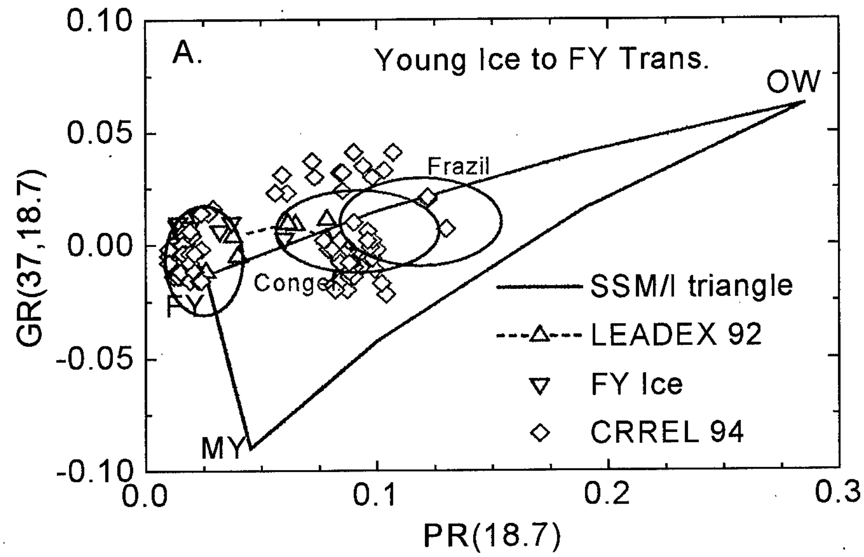

Fig. 2. Scatter plots PR versus GR for young ice and FY ice cases. The vertices of the triangle - OW, FY, and MY - refer to the assigned "tie points" for open water, first-year ice, and multiyear ice. Given in the legend are the sources for the various data sets. The ovals labeled "Congel." and "Frazil" give the location for observations of young congelation ice from five previous experiments and for observations of frazil ice from the CRREL 95 experiment respectively. The large triangle in A shows the region containing linear mixtures of open water (OW) FY ice and multiyear (MY) ice.

Scatter plots comparing emissivities at 18.7 and 37 GHz show tight clusters that are very similar in size and location to the bare ice results in figure 3. Comparisons of plots of these types can provides a useful way to detect the presence of snow on first-year ice. Unfortunately, these results are insensitive to snow thickness and depend more strongly on the degree of metamorphism in the snowpack. Since some researchers are presently using information of this sort to produce "snow thickness" maps from satellite imagery, further investigations into this topic would be advisable. For the case of multiyear ice, the ice itself can produce scattering and produces an effect similar to the snow cover in the 90 GHz emissivities, but in this case the clustering in an 18.7 versus 37GHz scatter plot does not resemble the picture in Figure 3. As a result, little can be deduced about snow cover on multiyear ice from this technique.

Figs. 4 and 5 are scatter plots showing the correlations of spectral albedo at 500 nm with selected emissivities from 1.4 to 90 GHz, backscattering coefficients from C- to Ka-band, α_λ at 400 nm, and thermal infrared (IR) emissivity. Almost all these quantities increase initially with increasing albedo as the thin ice develops, but the higher frequency microwave emissivities decrease with further albedo increases that arise from the addition of a snow layer. Values of σ^o level off for thicker ice although the introduction of snow increases the backscatter by several dB. The initial positive correlation is due to increases in bulk dielectric properties and the establishment of surface roughness. The negative correlation for millimeter wave emissivities is due to increased volume scattering in the snow as seen in σ^o.

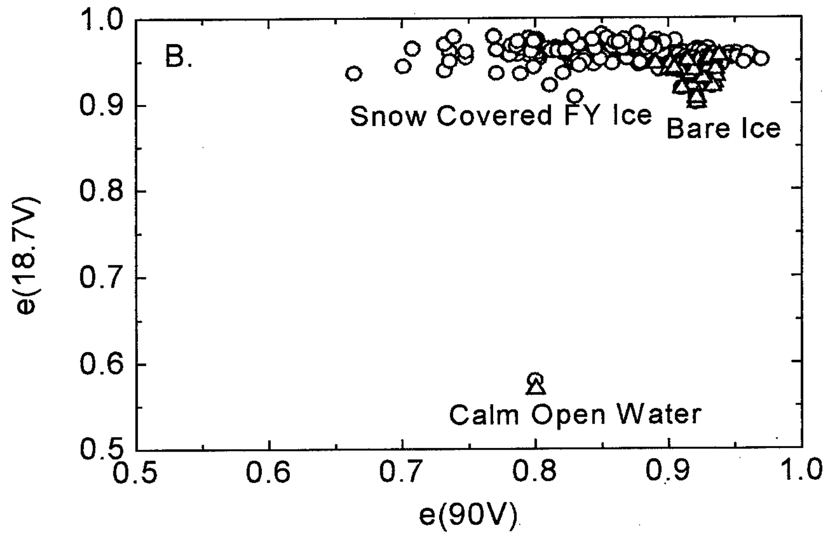

Fig. 3. Scatter plot e(18.7V) versus e(90V) for young ice and FY ice cases.

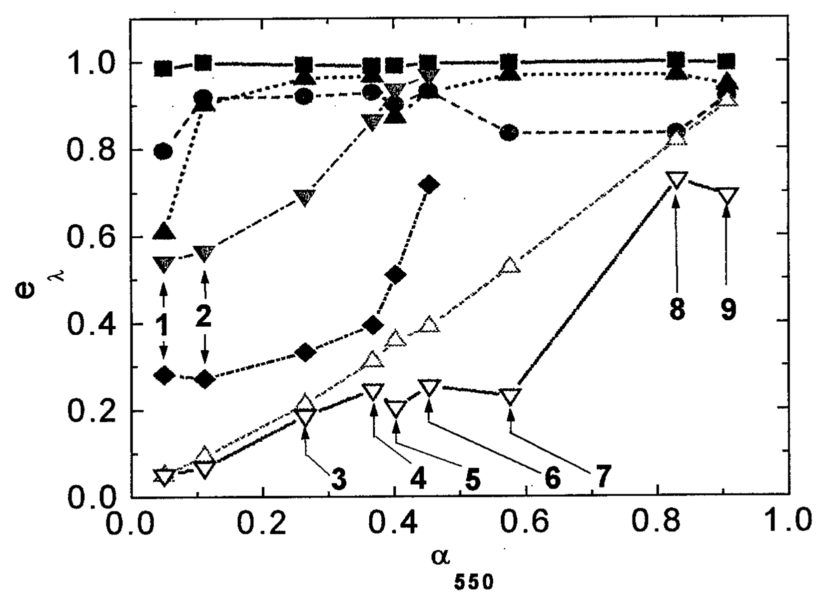

Fig. 4 Comparison of spectral albedo at 550 nm with selected microwave and thermal IR emissivities. Microwave emissivities include e(90V) filled circles, e(18.7V) filled up triangles, e(2.6V) filled down triangles, e(1.4H) filled diamonds. Infrared emissivity is indicated by the filled squares, α_{400} [open up triangles] and α_{1000} [open down triangles] versus α_{550} for all ice cases specified in Table 1.

TABLE 1 ICE/SNOW CHARACTERISTICS

Case	Ice Thickness	Snow Thickness	α_{550}
1	0 mm/ trace	0 mm	0.05
2	4 mm	0 mm	0.11
3	50 mm	0 mm	0.26
4	80 mm	0 mm	0.37
5	135 mm	0 mm	0.40
6	145 mm	20 mm	0.45
7	1.7 m	0 mm	0.58
8	0.31 m	85 mm	0.83
9	1.7 m	0.12 m	0.91

The situation with respect to the radar results is somewhat different. During new/young ice growth, $\sigma^o(25^o)$ increases with α_{550}, as do the microwave emissivities, and there is a strong correlation between σ^o and albedo; however, the correlation becomes very weak for the thicker ice types. This behavior is a result of changes in the surface roughness that occur throughout the growth and development of the ice. Saturation with respect to ice thickness occurs for z_{ice} slightly greater than 50 mm.

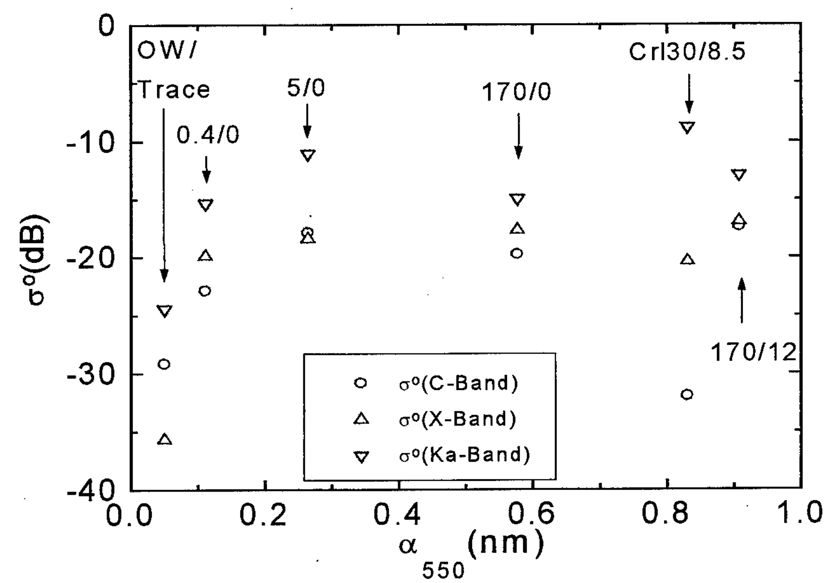

Fig. 5. Comparison of spectral albedo at 550 nm with microwave backscattering coefficients for selected ice and snow thickness. The ice thickness/snow thickness in cm are indicated as in Fig. 1.

For the thick and snow covered ice values of σ^o depend on how large the scatterers are and on the layer structure of the upper part of the ice and the snow. Case 8, for example, shows very low values of σ^o at C-band with a rapid increase at higher frequencies characteristic of a Rayleigh scattering response for a snow grain size that is small compared to the wavelength. Case 9, also a snow covered site, shows quite different behavior. Here our model results indicate that the snow acts as an impedence-matching layer because it contains a dielectric gradient due to vertical salinity and density gradients in the snow. This reduces the effective reflectivity of the system. As a result, PR decreases, as described above, and much of the radar wave is transmitted into the ice that would be backscattered if the dielectric discontinuity were more abrupt.

One conclusion that can be drawn from these comparisons is that there is no single detector or frequency that can be used as an effective proxy for sea ice albedo. Although this is probably possible over certain ranges of snow/ice conditions, it will in general be difficult to know for purposes of interpreting satellite imagery whether the appropriate physical conditions are present. This means that visible and/or near infrared radiance values can be used in conjunction with other sensor readings to obtain a more precise estimate of ice conditions.

Figs. 6 and 7 show comparisons of model results with observations for microwave emissivity and spectral albedo for selected cases. In both instances, we have been able to obtain a good match with the observations adhering to the constraints of the observations of the physical properties. Some refinements are indicated, however, such as the inclusion of surface roughness in the microwave model and absorption by foreign material such as chlorophyl, particulate material and dissolved matter in the visible-infrared model.

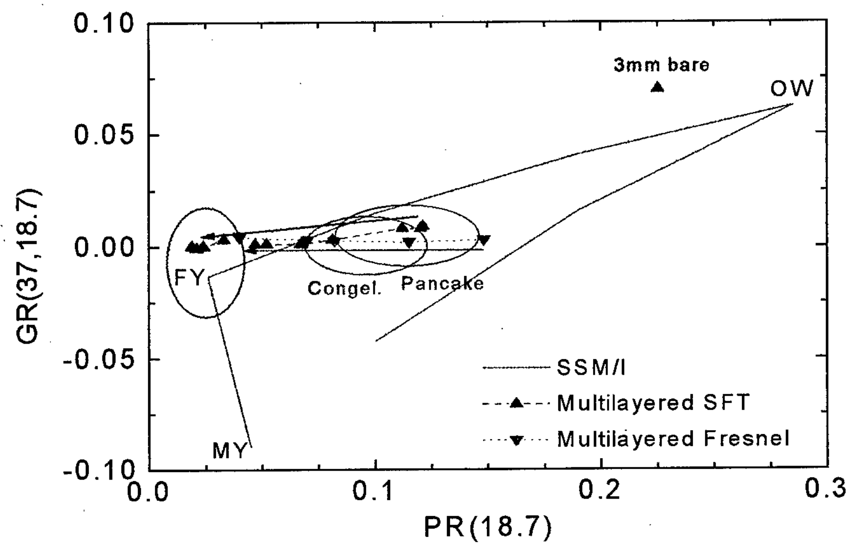

Fig. 6. Theoretical calculations of PR-GR evolution from young ice to thick first-year ice using mutilayer strong fluctuation theory (SFT) and Fresnel models.

For modeling the signature evolution, we find that proper representation of vertical structure is crucial and that multilayer models are required. In particular, the brine volume and bubble density profiles or grain size distribution must be represented accurately, so a single layer is not sufficient to represent either the ice or the snow. As many as 17 layers were used here to represent the brine volume profile adequately in the microwave model. Four layers were needed in the visible-infrared model to represent the vertical profile of particulates and dissolved material.

As shown in Figure 6 it was possible to model the evolution of PR and GR as young ice developed into FY ice. The crucial change was that a low density layer of snow or frost flowers must be deposited on the ice to produce PR values as low as 0.02.

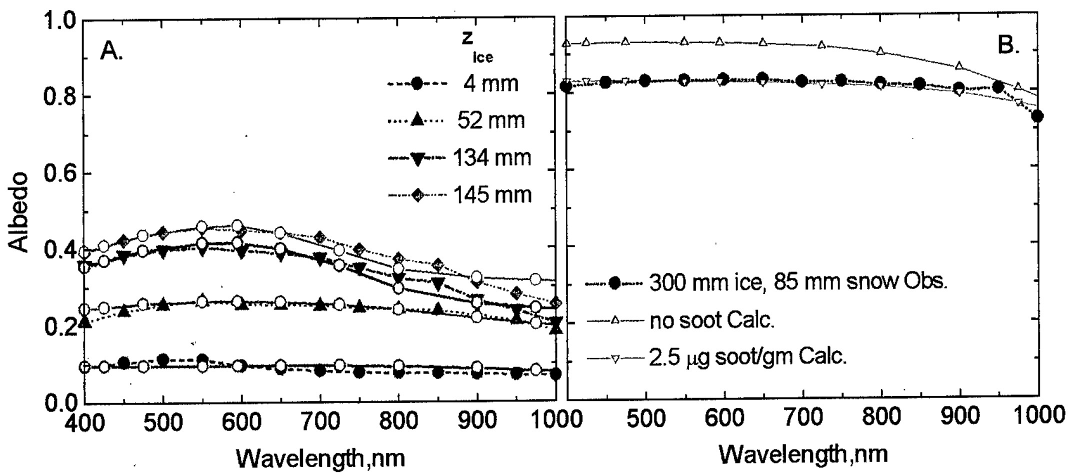

Fig. 7. Comparison of Radiative Transfer model calculations with spectral albedo observations versus ice and snow thickness: A. bare ice from 4 mm to 145 mm thickness; B. 300 mm thick ice with 85 mm snow and 85 mm of snow plus 2.5μg soot/gm.

Figure 7 shows that we were able to match the spectral albedos for both thin and thick FY ice types, however, measured impurities in the snow and ice were pivotal in obtaining agreement. Fortunately, impurity observations were provided for the thin ice cases by C. Roesler, and these are incorporated without modification into the calculations. In the case of the soot, we determined the amount of soot mixed uniformly into the snow needed to produce agreement. We conclude from this analysis that snow and ice in the Arctic Basin can be expected in general to contain levels of impurities from biological processes and from atmospheric deposition that are high enough to influence the spectral albedo significantly, and future programs should include appropriate measurements to determine impurity levels.

Thermal infrared (TIR) observations (Figure 8) show a much smaller dynamic range. Observationally significant differences in the emissivities were observed for different ice surface conditions as indicated. Because of the extremely high opacity of ice and water at TIR wavelengths, the emitted radiation originates only from a very thin layer at the surface. The emissivity is primarily influenced by the granularity or roughness of the surface. It was observed to be lowest for the smoothest surfaces (~0.98) and increased to well above 0.99 for rougher more complex surface types. One conclusion is that TIR measurements can be used effectively to determine surface temperatures with a precision of perhaps one degree Celsius in most cases, but care is required in interpretation because the temperature of the material at the surface can be influenced not only by local thermodynamic conditions but by advected heat during windy conditions. In the former case, considerable detail can be evident in TIR imagery while in the latter the detail can be smeared out completely.

On the basis of existing calculations of TIR emissivity for snow and ice surfaces, it appears that the model results are consistent with the present observations. However, a detailed match for specific structural conditions remains to be carried out.

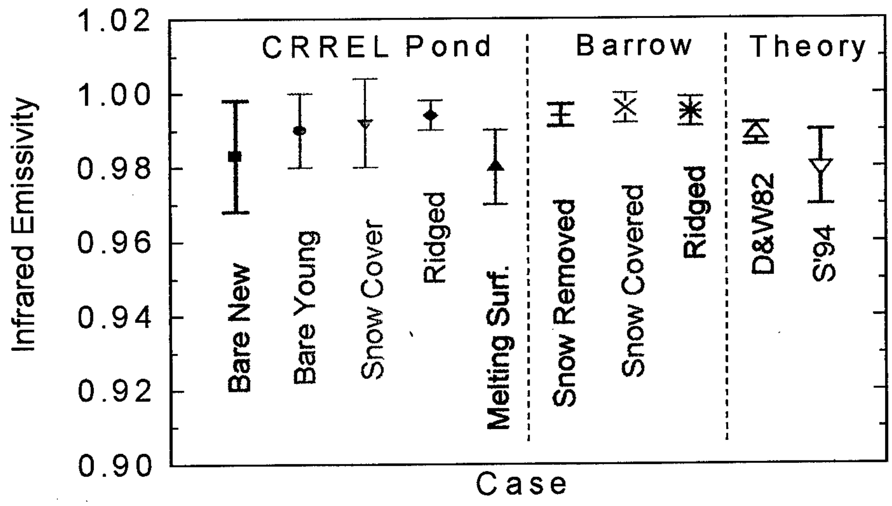

Fig. 8. Thermal infrared emissivities for the indicated ice types observed at 50° nadir angle at the CRREL Pond and at Barrow Alaska. Model results for snow are from Dozier and Warren. For pure ice they have been computed from the data of Salisbury *et al.*

IMPACT AND APPLICATIONS

Based on the work described above, our observations and modeling work have revealed several considerations which are central to understanding the physical basis for the application and interpretation of thin ice algorithms for passive microwave imagery. Our results have shown that passive microwave measurements provide one of the most robust remote sensing techniques for distinguishing among sea ice types - including the energetically important thin ice types. We have found that current theories applicable at microwave frequencies (multilayer SFT wave theory, for example) and in the visible and infrared (radiative transfer theory) can reproduce the radiation signatures of FY ice types quite well by incorporating the actual physical structure of the ice. As a result of the cooperative work carried out during the electromagnetics ARI, the determination of the wavelength regions and physical situations appropriate for the application of various models has been improved considerably, and our results, both theoretical and observational, have demonstrate the levels of accuracy of the models. It is clear that our understanding of the microwave emissivities of sea ice and their relation to other types of remote sensing signatures has increased significantly in the course of the ARI. The primary remaining limitation on passive microwave remote sensing is the coarse spatial resolution of the satellite imagery, and it is our primary recommendation that presently available aperture-synthesis techniques should be applied to building large satellite antennas to enhance the spatial resolution.

The techniques developed on this grant and the observational and modeling results from this project will be used in future research to determine the spatial and temporal distribution of the properties of sea ice. We plan to make direct use of these, for example, in the next two years as part of our involvement with SHEBA. We also anticipate that these results, currently submitted for publication, will have a significant impact on radar and visible/near-infrared remote sensing.

SELECTED PUBLICATIONS since 1993

Grenfell, T.C. and D.K. Perovich, 1993, Passive Microwave Study of Thin Sea Ice from the Arctic Lead Experiment, Abstract in PIERS 1993 Proceedings, 476.

Winebrenner, D.P., T.C. Grenfell, and M.R.Wensnahan, 1993, Modeling the Temporal Evolution of L-Band Polarimetric SAR Observations of Growing Sea Ice in Arctic Leads, Abstract in PIERS 1993 Proceedings, 478.

Grenfell, T. C., J. C. Comiso, M. A. Lange, H. Eicken, M. R. Wensnahan, 1994, Passive microwave observations of the Weddell Sea during austral winter and early spring, *J. Geophys. Res.*, *99*, 9,995-10,010.

Grenfell, T.C., M.R. Wensnahan, and D.P. Winebrenner, Passive microwave signatures of simulated pancake ice and young pressure ridges, *Remote Sensing Rev.*, Vol. 9, pp. 51-64, 1994.

Grenfell, T.C., and D.K. Perovich, 1994, Analysis of Surface-Based Passive Microwave Observations during LEADEX 1992, Proceedings of IGARSS '94, 1005-1007.

Grenfell, T.C., M.R. Wensnahan, and D.P. Winebrenner, 1994, Measurements of Microwave Emission from New and Young Saline Ice during the 1993 CRREL Pond Experiment, IGARSS '94 Proceedings, 605-607.

Lohanick, A.W., and T.C. Grenfell, Snow Cover Characterization, 1994, EMPOSI 94 Field Experiment at Barrow Alaska, Data Report.

Grenfell, T.C., M.R. Wensnahan, D.P. Winebrenner and L. Zurk, 1995:Passive Microwave and Infrared Observations of New and Young Sea Ice - The 1994 CRREL Pond Experiment, Abstract in PIERS 1995 Proceedings, 66.

Grenfell, T.C., D.P. Winebrenner and A. W. Lohanick, 1995, Passive Microwave and Thermal Infrared Emissivities of First-Year Sea Ice Near Point Barrow Alaska, Abstract in PIERS 1995 Proceedings, 479.

Podgorny, I.A., and T.C. Grenfell, 1996, Partitioning of Solar Energy in Melt Ponds from Measurements of Pond Albedo and Depth, *J. Geophys. Res.*, 101, 22,737-22,748.

Podgorny, I.A., and T.C. Grenfell, 1996, Absorption of solar energy in a cryoconite hole, *Geophys. Res. Letters*, *23*, 2465-2468.

Grenfell, T. C., Microwave and thermal infrared emission from young sea ice and pancake ice, Proceedings of IGARSS '96, 1199-1201, 1996.

Wensnahan, M.R., T.C. Grenfell, G.A. Maykut and D.P. Winebrenner, Physical properties affecting the passive microwave signature of thin sea ice, *J. Geophys. Res.*, submitted.

Wensnahan, M.R., G.A. Maykut, T.C. Grenfell and D.P. Winebrenner, Predicting geophysical parameters associated with thin sea ice from passive microwave satellite data, *J. Geophys. Res.*, submitted.

Light, B., H. Eicken, G.A. Maykut, and T.C. Grenfell, 1997, A Model study of the effect of particulates on the albedo sea ice, *J. Geophys. Res.*, submitted.

Nghiem, S. V., R. Kwok, S. H. Yueh, A. J. Gow,.D. K. Perovich, C. C. Hsu, K. H. Ding., J. A. Kong, T. C. Grenfell, Diurnal thermal cycling effects on backscatter and emissivity of thin sea ice, *IEEE TGRS*, 36, No.1, ,1998.

Furhop, R. and others, A combined radiative transfer model for sea ice, open ocean, and atmosphere, *Intl. J. Rem. Sens.*, submitted.

Grenfell, T. C. and others, Evolution of the electromagnetic signatures of young sea ice Part 1 initial growth, IEEE TGRS submitted.

Grenfell, T. C. and others, Evolution of the electromagnetic signatures of young sea ice Part 2 The onset of melting, IEEE TGRS, submitteed.

Perovich, D. K. and others, Passive Microwave and Thermal Infrared Emissivities of First Year Sea Ice at Point Barrow, Alaska, IEEE TGRS, submitted.

Onstott, R. G. and others, Development of the electromagnetic signatures of frazil/pancake ice - a comparison with congelation ice, IEEE TGRS, submitted.

Barber, D.G. and others, The role of snow cover on sea ice in determining electromagnetic interactions over the range 0.4 microns to 5 cm, IEEE TGRS, submitted.
Mobley, K. and others, Radiative transfer modeling of sea ice, IEEE TGRS, submitted.
Golden, K. and others, Forward models of the electromagnetic properties of sea ice, IEEE TGRS, submitted.
Jezek, K. A. and others, An overview of the ONR electromagnetics ARI program, IEEE TGRS, submitted.